Low Energy Three- and Four-Body Systems in EFTs

S@INT Oct. 24, 2023

Xincheng Lin
Duke University

Overview

Overarching goals:

- Manifestation of QCD in terms of hadrons and/or nuclei using EFTs
- Understanding how nuclear physics arises from QCD

Pionless EFT in three-body systems and approximate symmetries:

- Wigner-SU(4) symmetry
  - Cold neutron-deuteron radiative capture
- Large N_c expansion
  - Dark matter (DM) scattering off light nuclei

Four-body systems

- Renormalization group (RG) behavior of four-body observables
  - Role of three-body Efimov states

Motivation

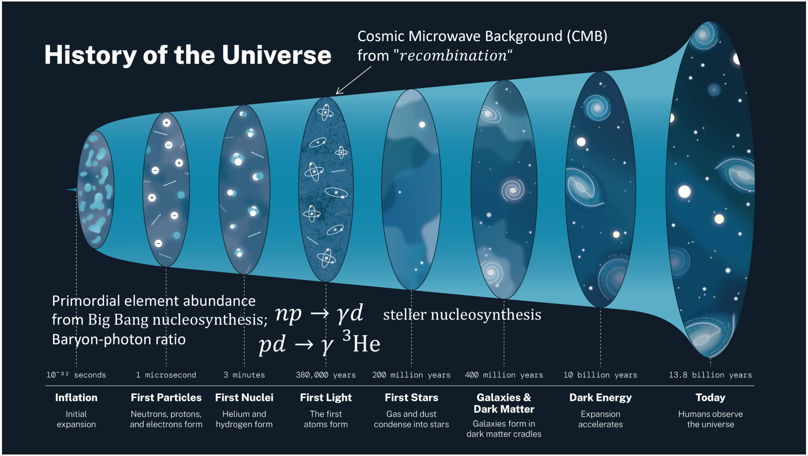

Figure 1: Source: https://universe.nasa.gov/universe/basics/

Motivation

$pd \to \gamma\ ^3\text{He}$

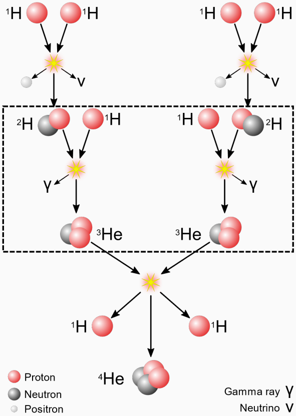

Big Bang nucleosynthesis
$p_{nuc} < \gamma_t = 45.7$ MeV

Temperature in the Sun's core
$\approx 1.5 \times 10^7$ Kelvin
≈ 1.3 keV
$\to p_{nuc} \sim 1$ MeV

Thermal proton/neutron speed
≈ 2200 m/s
$\to\ p_{nuc} \sim 5$ keV

Figure 2: Proton-Proton chain. Source:
https://en.wikipedia.org/wiki/Proton%E2%80%93proton_chain#/media/File:Fusion_in_the_Sun.svg

Pioneless EFT

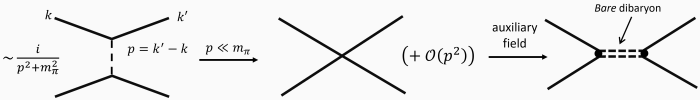

- Expansion parameter: $Q \sim \frac{M_{\text{low}}}{M_{\text{high}}} \sim \frac{\gamma_t}{m_\pi} \approx \frac{1}{3}$
- LO two-nucleon interactions and low-energy coefficients (LECs) in the partial wave basis:

$$C^{\,^3S_1}\left(N^T\mathcal{P}_i^{\,^3S_1}N\right)^\dagger\left(N^T\mathcal{P}_i^{\,^3S_1}N\right), \qquad C^{\,^1S_0}\left(N^T\mathcal{P}_a^{\,^1S_0}N\right)^\dagger\left(N^T\mathcal{P}_a^{\,^1S_0}N\right)$$

- Sum over all diagrams of the same order and match LECs to two-body poles:

$$C^{\,^3S_1} = \frac{4\pi}{m_N}\frac{1}{\gamma_t - \mu}, \qquad C^{\,^1S_0} = \frac{4\pi}{m_N}\frac{1}{\gamma_s - \mu},$$

μ: subtraction point in power divergence subtraction scheme (*Kaplan, Savage, and Wise 1998*);
$\mu \sim$ linear divergence from two-body loop diagram in three-spatial dimension.

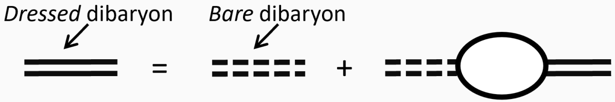

Figure 3: Geometric sum for dressed dibaryon

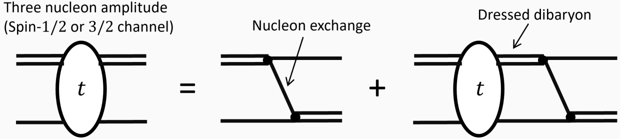

Figure 4: Three-body integral equation for scattering amplitude. Equivalent to Faddeev equation.

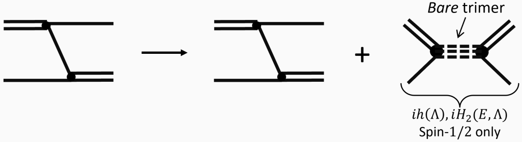

Figure 5: Three-body force (*P. Bedaque, Hammer, and van Kolck 1999; P. F. Bedaque, Rupak, Grießhammer, and Hammer 2003*)

Dressed Trimer and Trimer Vertex Function

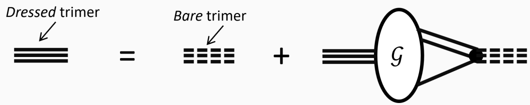

Figure 6: Geometric sum for dressed trimer

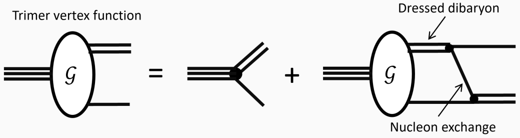

Figure 7: Integral equation for trimer vertex function

- Dressed trimer propagator can be used to calculate three-body force and trimer wavefunction renormalization factor
- Trimer vertex function $\mathcal{G}$ is needed in any calculation involving a three-body bound state (e.g., form factor, breakup, elastic scatterings)

Mom, I wanna have my dessert of $pd \to \gamma\ {}^3\mathrm{He}$

Not until you finish up your meal of $nd \to \gamma\ {}^3\mathrm{H}$

Cold radiative *nd* Capture

(*Lin, Singh, Springer, and Vanasse 2023*)

- Necessary for studying proton-deuteron capture
- Five parity-violating (PV) interactions at LO in pionless EFT for two and three nucleons. PV observables in *nd* and *pd* capture? (See pionless EFT study of PV in *np* capture by *Schindler and Springer 2010* and in *nd* scattering by *Vanasse 2012*)
- Approximate symmetries, power counting, renormalization group (RG) behavior
- Numerical and analytical method for more complicated processes, e.g., proton-deuteron capture, four-nucleon systems with external currents.

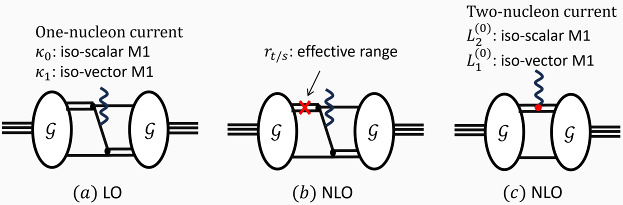

Figure 8: Example diagrams for trimer form factor

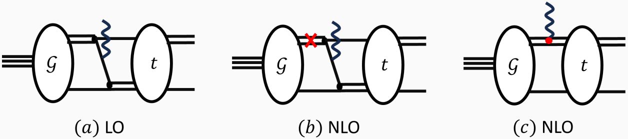

Figure 9: Example diagrams for trimer breakup.

Three-Nucleon Systems: Observables up to NLO

	LO $\left(\mathcal{O}(Q^0)\right)$	NLO $\left(\mathcal{O}(Q^1)\right)$
Strong interactions	$\gamma_{t/s}$, $h(\Lambda)$	$r_{t/s}$
M1 transitions	κ_0, κ_1	$L_1^{(0)}, L_2^{(0)}$
σ_{np} [mb], exp $= 334.2(5)$	325.2	$22.1 + 27.3\left(L_1^{(0)}\text{ [fm]} + 6.41\right)$
$\mu_{^3\text{H}}\left[\frac{e}{2m_N}\right]$, exp $= 2.98$	2.75	$0.03 + 0.28\left(L_1^{(0)}\text{ [fm]} + 6.41\right)$
σ_{nd} [mb], exp $= 0.508(15)$	0.31	$-0.07 + 0.13\left(L_1^{(0)}\text{ [fm]} + 6.41\right)$

Table 1: Parameters and observables with M1 transitions. σ_{np} and $\mu_{^3\text{H}}$ are calculated by *Chen, Rupak, and Savage 1999* and *Vanasse 2018*, respectively. σ_{nd} is from our calculation *Lin, Singh, Springer, and Vanasse 2023*.

	LO $\left(\mathcal{O}(Q^0)\right)$	NLO $\left(\mathcal{O}(Q^1)\right)$
σ_{np} [mb], exp = 334.2(5)	325.2	$22.1 + 27.3\left(L_1^{(0)}\,[\text{fm}] + 6.41\right)$
$\mu_{^3\text{H}}\left[\frac{e}{2m_N}\right]$, exp = 2.98	2.75	$0.03 + 0.28\left(L_1^{(0)}\,[\text{fm}] + 6.41\right)$
σ_{nd} [mb], total	0.31	$-0.07 + 0.13\left(L_1^{(0)}\,[\text{fm}] + 6.41\right)$
σ_{nd} [mb], Spin=$\frac{1}{2}$	0.16	$0.01 + 0.16\left(L_1^{(0)}\,[\text{fm}] + 6.41\right)$
σ_{nd} [mb], Spin=$\frac{3}{2}$	0.15	$-0.08 - 0.035\left(L_1^{(0)}\,[\text{fm}] + 6.41\right)$

Table 2: Parameters and observables with M1 transitions. σ_{np} and $\mu_{^3\text{H}}$ are calculated by *Chen, Rupak, and Savage 1999* and *Vanasse 2018*, respectively.

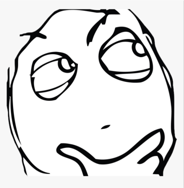

Is pionless EFT expansion alone sufficient to understand nd capture?

Wigner-SU(4) Symmetry

Background:

- Approximate symmetry of nuclear interactions with four degrees of freedom $(p\uparrow, p\downarrow, n\uparrow, n\downarrow)$
- First studied by *Wigner 1937*
- Recent lattice results using Wigner-SU(4) symmetric nuclear interactions given by *Lu et al. 2019*

Example of two-nucleon interactions at LO:

- In the Wigner basis:

$$C_I\left(N^\dagger N\right)^2, \quad C_\sigma\left(N^\dagger \sigma^i N\right)^2, \quad C_\tau\left(N^\dagger \tau^a N\right)^2, \quad C_{\sigma\tau}\left(N^\dagger \sigma^i \tau^a N\right)^2$$

- Two independent interactions (Fierz identities):

$$-\tfrac{1}{2}\widetilde{C}_I\left(N^\dagger N\right)^2, \quad -\tfrac{1}{2}\widetilde{C}_\sigma\left(N^\dagger \sigma^i N\right)^2$$

Wigner-SU(4) Symmetry

Example of two-nucleon interactions at LO:

- In the Wigner basis:

$$C_I \left(N^\dagger N\right)^2, \quad C_\sigma \left(N^\dagger \sigma^i N\right)^2, \quad C_\tau \left(N^\dagger \tau^a N\right)^2, \quad C_{\sigma\tau} \left(N^\dagger \sigma^i \tau^a N\right)^2$$

- Two independent interactions (Fierz identities):

$$-\tfrac{1}{2}\widetilde{C}_I \left(N^\dagger N\right)^2, \quad -\tfrac{1}{2}\widetilde{C}_\sigma \left(N^\dagger \sigma^i N\right)^2$$

- Transform to partial wave basis:

$$C^{\,{}^3S_1} = \widetilde{C}_I - 3\widetilde{C}_\sigma, \quad C^{\,{}^1S_0} = \widetilde{C}_I + \widetilde{C}_\sigma$$

- $\widetilde{C}_\sigma$ breaks Wigner-SU(4) symmetry. ***In the Wigner-SU(4) limit***, $\widetilde{C}_\sigma \to 0$, which means

$$C^{{}^3S_1} = C^{{}^1S_0} \longrightarrow \gamma_t = \gamma_s$$

Some intuition about Wigner-SU(4) symmetry:

- Cancellation of e.g., spin-dependent forces
- Relates nuclear systems to bosonic systems, e.g., three-nucleon system and three-boson system
- Emerges (*Kaplan and Savage 1996*) in the limit of large number of QCD colors (large N_c limit)

In the Wigner-SU(4) limit, we take

$$\gamma_{t/s} \to \gamma = \frac{1}{2}\left(\gamma_t + \gamma_s\right), \qquad r_{t/s} \to r = \frac{1}{2}\left(r_t + r_s\right) \tag{1}$$

In the Wigner-SU(4) limit, we take

$$\gamma_{t/s} \to \gamma = \frac{1}{2}\left(\gamma_t + \gamma_s\right), \qquad r_{t/s} \to r = \frac{1}{2}\left(r_t + r_s\right) \tag{1}$$

Parameterization of Wigner-SU(4) breaking:

$$\delta = \frac{1}{2}\left(\gamma_t - \gamma_s\right), \qquad \delta_r = \frac{1}{2}\left(r_t - r_s\right) \tag{2}$$

Relative sizes of the Wigner-SU(4) breaking:

$$\frac{\delta}{\gamma} \approx 50\%, \qquad \frac{\delta_r}{r} \approx 10\% \sim Q^2 \tag{3}$$

Wigner-SU(4) Symmetry: Parameterizations

In the Wigner-SU(4) limit, we take

$$\gamma_{t/s} \to \gamma = \frac{1}{2}\left(\gamma_t + \gamma_s\right), \qquad r_{t/s} \to r = \frac{1}{2}\left(r_t + r_s\right) \tag{1}$$

Parameterization of Wigner-SU(4) breaking:

$$\delta = \frac{1}{2}\left(\gamma_t - \gamma_s\right), \qquad \delta_r = \frac{1}{2}\left(r_t - r_s\right) \tag{2}$$

Relative sizes of the Wigner-SU(4) breaking:

$$\frac{\delta}{\gamma} \approx 50\%, \qquad \frac{\delta_r}{r} \approx 10\% \sim Q^2 \tag{3}$$

- Two-nucleon systems and ***three-nucleon scatterings at low energies***: generally ***non-perturbative in*** δ, but perturbative in δ_r which enters at N^3LO.

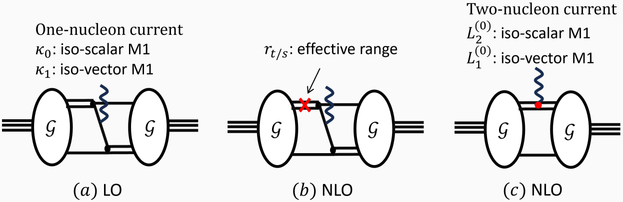

Figure 10: Example diagrams for trimer form factor

Q: What about three-body bound states? Is it perturbative in δ?

A: Yes! $\sim$ 10% ***correction from*** δ**.**(*Vanasse and Phillips 2017; Vanasse 2018*).

Wigner-SU(4) Symmetry: Three-Body Bound State Properties

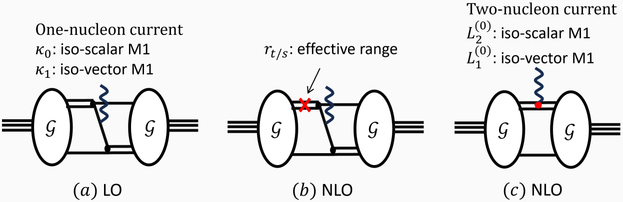

Figure 10: Example diagrams for trimer form factor

Q: What about three-body bound states? Is it perturbative in δ?

A: Yes! $\sim$ 10% ***correction from*** δ.(*Vanasse and Phillips 2017; Vanasse 2018*).

- Wigner-SU(4) symmetry and separation between two- and three-body scales
- Triton vertex function dominated ($\sim$ 90%) by Wigner-SU(4) symmetric part

Wigner-SU(4) Symmetry: Three-Body Bound State Properties

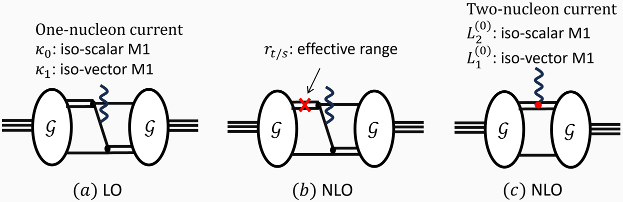

Figure 10: Example diagrams for trimer form factor

Q: What about three-body bound states? Is it perturbative in δ?
A: Yes! $\sim$ 10% ***correction from*** δ.(*Vanasse and Phillips 2017; Vanasse 2018*).

- Wigner-SU(4) symmetry and separation between two- and three-body scales
- Triton vertex function dominated ($\sim$ 90%) by Wigner-SU(4) symmetric part

In the limit of Wigner-SU(4) symmetry (*Vanasse 2018*),

$$\mu_{^3\mathrm{H}}^{\mathrm{LO}} = \left\langle {}^3\mathrm{H} \middle| \sum_{i=1}^{3} \left(\kappa_0 + \kappa_1 \tau^i\right) \sigma^i \middle| {}^3\mathrm{H} \right\rangle = \kappa_0 + \kappa_1 = \mu_p = 2.79 \left[\frac{e}{2m_N}\right], \tag{4}$$

to be compared with $\mu_{^3\mathrm{H}}^{\mathrm{exp}} = 2.98$ and $\mu_{^3\mathrm{H}}^{\mathrm{LO}} = 2.75$ with physical paramters.

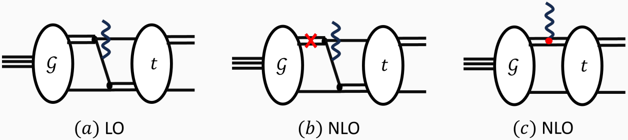

Figure 11: Example diagrams for trimer form factor

Q: What about neutron-deuteron capture?

A: Although t is not perturbative in δ (δ/p_n), in the limit of Wigner-SU(4) symmetry we have

$$A_{nd}^{\text{LO}} = \langle nd| \sum_{i=1}^{3} \left(\kappa_0 + \kappa_1 \tau^i\right) \sigma^i \left|{}^3\text{H}\right\rangle = (\kappa_0 + \kappa_1) \left\langle nd\middle|{}^3\text{H}\right\rangle = 0, \tag{5}$$

which explains why σ_{nd} is so small at LO!

Q: Is pionless EFT expansion alone sufficient to understand *nd* capture?

A: No, we also need the approximate Wigner-SU(4) symmetry.

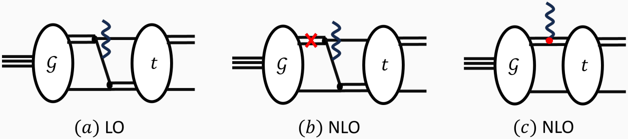

Figure 11: Example diagrams for trimer form factor

Q: Higher orders and multi-nucleon currents?

A: That's tricky. **At NLO**,

- ***in the Wigner-SU(4) limit***, two-body currents not required for RG invariance, $\sigma_{nd}^{\mathrm{NLO}} = 0$;

Wigner-SU(4) Symmetry: *nd* Capture with M1 Transitions

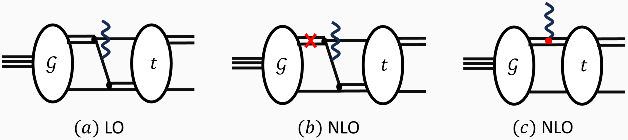

Figure 11: Example diagrams for trimer form factor

Q: Higher orders and multi-nucleon currents?

A: That's tricky. **At NLO**,

- ***in the Wigner-SU(4) limit***, two-body currents not required for RG invariance, $\sigma_{nd}^{\mathrm{NLO}} = 0$;
- ***in the physical limit***, two-body current needed for RG invariance and fit to other observables. *nd* capture can be ***sensitive to two-body currents***.

Wigner-SU(4) Symmetry: *nd* Capture with M1 Transitions

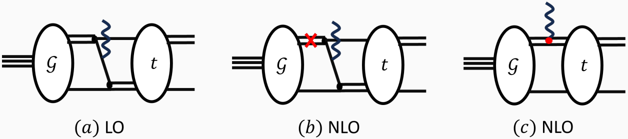

Figure 11: Example diagrams for trimer form factor

Q: Higher orders and multi-nucleon currents?

A: That's tricky. **At NLO**,

- ***in the Wigner-SU(4) limit***, two-body currents not required for RG invariance, $\sigma_{nd}^{\text{NLO}} = 0$;
- ***in the physical limit***, two-body current needed for RG invariance and fit to other observables. *nd* capture can be ***sensitive to two-body currents***.

At NNLO,

- Orthogonality does not work for energy-dependent three-body force $H_2(E, \Lambda)$ (see, e.g., *Formánek, Lombard, and Mareš 2004*)$\rightarrow$ enhanced contribution from $H_2(E, \Lambda)$
- ***More divergence***

nd Capture: Combined Pionless EFT and Wigner-SU(4) Expansion

- Pionless EFT expansion alone:

Contribution from n-nucleon current

$$A_{nd} = A_{Q^0}^{(1)} + \sum_{n=1,2} A_{Q^1}^{(n)} + \sum_{n=1,2,3} A_{Q^2}^{(n)} + \cdots$$

Power counting in pionless EFT

- Wigner-SU(4) expansion for the LO term: $\delta_w = \delta/\kappa_3^*$, where κ_3^* is a three-body scale:

$$A_{Q^0}^{(1)} = \underbrace{A_{Q^0\,\delta_w^0}^{(1)}}_{0} + A_{Q^0\,\delta_w^1}^{(1)} + \cdots$$

- Combined expansion (superscript H_2 indicates contribution from $H_2(E,\Lambda)$):

$$A_{nd} = \begin{cases} \underbrace{0}_{\mathcal{O}(Q^0)} + \underbrace{A_{Q^0\,\delta_w^1}^{(1)}}_{\mathcal{O}(Q^1)} + \underbrace{\left(A_{Q^1\,\delta_w^1}^{(1)} + A_{Q^2\,\delta_w^0}^{(1,\,H_2)} + A_{Q^1\,\delta_w^1}^{(2)} + A_{Q^2\,\delta_w^0}^{(3)}\right)}_{\mathcal{O}(Q^2)}, & \text{if } \delta_w \sim Q \\ \underbrace{0}_{\mathcal{O}(Q^0)} + \underbrace{0}_{\mathcal{O}(Q^1)} + \underbrace{\left(A_{Q^0\,\delta_w^1}^{(1)} + A_{Q^2\,\delta_w^0}^{(1,\,H_2)} + A_{Q^2\,\delta_w^0}^{(3)}\right)}_{\mathcal{O}(Q^2)}, & \text{if } \delta_w \sim Q^2 \end{cases}$$

	LO $\left(\mathcal{O}(Q^0)\right)$	NLO $\left(\mathcal{O}(Q^1)\right)$	NNLO $\left(\mathcal{O}(Q^2)\right)$
Strong interactions	$\gamma_{t/s}$ (2N) $h(\Lambda)$ (3N)	$r_{t/s}$ (2N)	$H_2(E,\Lambda)$ (3N)
M1 transitions	κ_0, κ_1 (1N)	$L_1^{(0)}, L_2^{(0)}$ (2N)	$L_1^{(1)}, L_2^{(1)}$ (2N) ? (3N)

Table 3: Parameters up to NNLO

Figure 12: Cutoff dependence of NNLO correction to triton magnetic moment ***without three-nucleon magnetic moment counterterm***

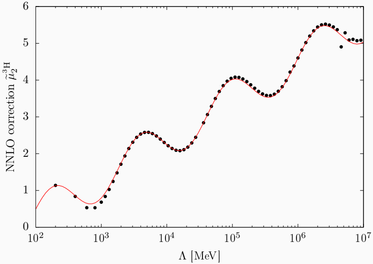

Figure 13: Counterterm needed to renormalize $\mu_{^3\mathrm{H}}$ at NNLO. $\widetilde{\kappa}_0(\Lambda) - \widetilde{\kappa}_1(\Lambda)$ is fit to $\mu_{^3\mathrm{H}}^{\mathrm{exp}}$.

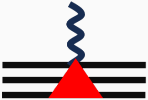

$\tilde{\kappa}_0(\Lambda)$: iso-scalar M1
$\tilde{\kappa}_1(\Lambda)$: iso-vector M1

nd Capture: Cutoff Dependence at NNLO

	LO $\left(\mathcal{O}(Q^0)\right)$	NLO $\left(\mathcal{O}(Q^1)\right)$	NNLO $\left(\mathcal{O}(Q^2)\right)$
Strong interactions	$\gamma_{t/s}$ (2N) $h(\Lambda)$ (3N)	$r_{t/s}$ (2N)	$H_2(E,\Lambda)$ (3N)
M1 transitions	κ_0, κ_1 (1N)	$L_1^{(0)}, L_2^{(0)}$ (2N)	$L_1^{(1)}, L_2^{(1)}$ (2N) $\widetilde{\kappa}_0(\Lambda), \widetilde{\kappa}_1(\Lambda)$ (3N)

Table 4: Parameters up to NNLO

Figure 14: Counterterm needed to renormalize σ_{nd} at NNLO. $\widetilde{\kappa}_0(\Lambda) - \widetilde{\kappa}_1(\Lambda)$ is fit to $\mu_{^3\mathrm{H}}^{\mathrm{exp}}$.

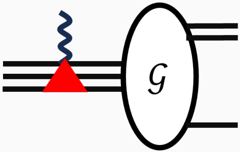

$\tilde{\kappa}_0(\Lambda)$: iso-scalar M1

$\tilde{\kappa}_1(\Lambda)$: iso-vector M1

Figure 15: Cutoff dependence of $\sigma_{nd}^{\mathrm{NNLO}}$ including $\widetilde{\kappa}_0(\Lambda) - \widetilde{\kappa}_1(\Lambda)$.

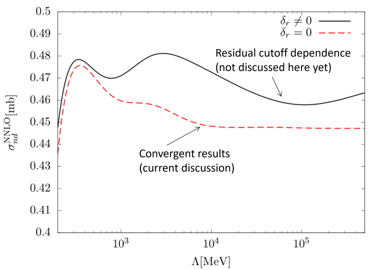

nd Capture: Sensitivity to Two-Nucleon Currents and Results

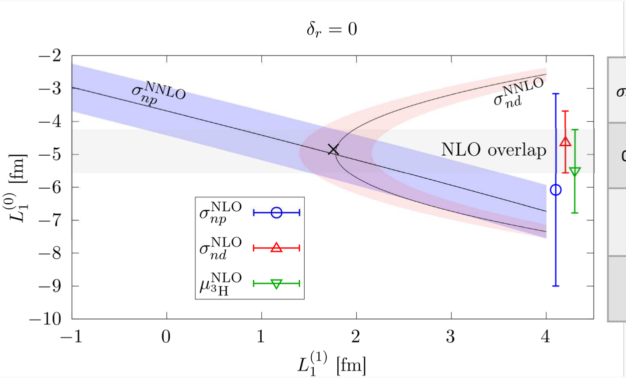

σ_{nd}^{NNLO}[mb]	$L_1^{(0)}$ fit	$L_1^{(1)}$ fit
0.447[130]	$\mu_{^3H}^{exp}$	σ_{np}^{exp}
0.511(42)	$\mu_{^3H}^{exp}, \sigma_{nd}^{exp}, \sigma_{np}^{exp}$	$\sigma_{nd}^{exp}, \sigma_{np}^{exp}$
exp. 0.508(15)		

Figure 16: Correlation between $L_1^{(0)}$ and $L_1^{(1)}$. Error bars (colored regions) represent naive pionless EFT error at NLO (at NNLO) for each observable. "NLO overlap" represents the range of $L_1^{(0)}$ that reproduces all three observables within NLO error. "×" is the best fit to all three observables at NNLO. Table shows σ_{nd}^{NNLO} for two different fittings.

- High sensitivity of σ_{nd}^{NLO} to $L_1^{(0)}$ is reflected by the red error bar being much shorter.

nd Capture: Sensitivity to Two-Nucleon Currents and Results

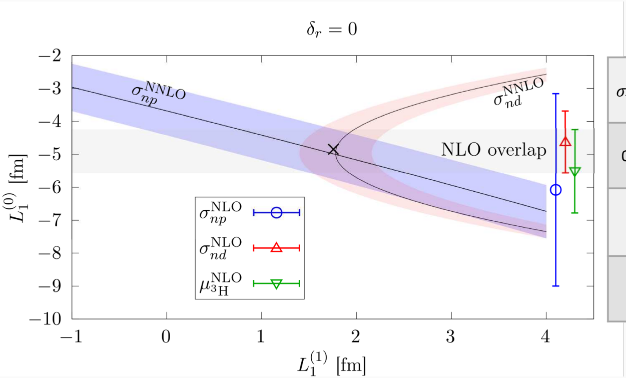

$\sigma_{nd}^{\mathrm{NNLO}}$[mb]	$L_1^{(0)}$ fit	$L_1^{(1)}$ fit
0.447[130]	$\mu_{^3\mathrm{H}}^{\mathrm{exp}}$	$\sigma_{np}^{\mathrm{exp}}$
0.511(42)	$\mu_{^3\mathrm{H}}^{\mathrm{exp}}, \sigma_{nd}^{\mathrm{exp}}, \sigma_{np}^{\mathrm{exp}}$	$\sigma_{nd}^{\mathrm{exp}}, \sigma_{np}^{\mathrm{exp}}$
exp. 0.508(15)		

Figure 16: Correlation between $L_1^{(0)}$ and $L_1^{(1)}$. Error bars (colored regions) represent naive pionless EFT error at NLO (at NNLO) for each observable. "NLO overlap" represents the range of $L_1^{(0)}$ that reproduces all three observables within NLO error. "×" is the best fit to all three observables at NNLO. Table shows $\sigma_{nd}^{\mathrm{NNLO}}$ for two different fittings.

- High sensitivity of $\sigma_{nd}^{\mathrm{NLO}}$ to $L_1^{(0)}$ is reflected by the red error bar being much shorter.
- At NLO there exists an overlap among all three error bars.
- At NNLO there exists an overlap among all shaded regions.

Large N_c Expansion

- Additional symmetry for SU(N_c) gauge theory in the limit $N_c \to \infty$, where N_c is the number of colors in QCD, and use $1/N_c$ as an expansion parameter (*'t Hooft 1974; Witten 1979*).
- Constrain relative sizes of LECs of nucleon interactions (*Kaplan and Savage 1996*) at a given EFT order $\to$ increase predictive power of combined EFT-large-N_c expansion
- Very useful when data is insufficient to fit all LECs at a given EFT order, e.g., parity violation (*Schindler, Springer, and Vanasse 2016*), DM-light-nuclei elastic scatterings (*Richardson, Lin, and Nguyen 2022*)

Large N_c Expansion

1. Single-baryon matrix element of m-quark operators (*Dashen, Jenkins, and Manohar 1995*):

$$\langle B'|\mathcal{O}^{(m)}_{I,S}/N_c^m|B\rangle \lesssim N_c^{-|I-S|}, \qquad S: \text{spin}, \ I: \text{isospin} \tag{6}$$

2. Two-nucleon matrix element factorizes in the large-N_c limit (*Kaplan and Savage 1996*):

$$\langle N_\alpha N_\beta|\mathcal{O}_1\mathcal{O}_2|N_\gamma N_\delta\rangle \xrightarrow{N_c\to\infty} \langle N_\alpha|\mathcal{O}_1|N_\gamma\rangle\langle N_\beta|\mathcal{O}_2|N_\delta\rangle + \text{cross term} \tag{7}$$

3.1 Scalings of (overcomplete) LO LECs in pionless EFT, for example:

$$C_I, C_{\sigma\tau} \sim O(N_c), \quad C_\sigma, C_\tau \sim O\left(\frac{1}{N_c}\right) \tag{8}$$

3.2 Set of independent LECs (caution!):

$$\widetilde{C}_I \sim O(N_c), \quad \widetilde{C}_\sigma \sim O\left(\frac{1}{N_c}\right) \tag{9}$$

4. Transform to partial wave basis

$$C^{^3S_1} = \widetilde{C}_I - 3\widetilde{C}_\sigma \tag{10}$$

$$\overset{N_c\to\infty}{=} C^{^1S_0} = \widetilde{C}_I + \widetilde{C}_\sigma \tag{11}$$

Application: Dark Matter Scattering off Light Nuclei

(*Richardson, Lin, and Nguyen 2022*)

- Large N_c scaling of for single- and two-nucleon-WIMP (spin $= 1/2$) operators
- Combined Pionless-EFT-large-N_c expansion for DM-light-nuclei (up to ^{3}H/^{3}He) elastic scatterings
- Useful for understanding the character of DM with future DM direct detection experiment using ^{3}He/^{4}He as targets

Large N_c scaling of single-nucleon-DM current can be obtained using the scaling of single-baryon matrix element. To get the scaling of two-nucleon-DM matrix element $\langle N_\alpha N_\beta \chi | \mathcal{O}_{\chi NN} | N_\gamma N_\delta \chi \rangle$, we assume (*Richardson and Schindler 2020*)

- nucleonic part takes a Hartree form, just like the nucleon-nucleon interaction, in the large N_c limit
- nucleonic part factorizes in the large N_c limit

Large N_c scaling is then obtained in a similar manner to nucleon-nucleon interactions, e.g.,

$$\mathcal{L}_{\chi NN} = \left(\chi^\dagger \chi\right) \Big[C_{1,\chi NN} \left(N^\dagger N\right)^2 + C_{2,\chi NN} \left(N^\dagger \sigma^i N\right)^2 + C_{3,\chi NN} \left(N^\dagger \tau^a N\right)^2 + C_{4,\chi NN} \left(N^\dagger \sigma^i \tau^a N\right)^2 \Big] \tag{12}$$

LECs scale as

$$C_{1,\chi NN},\ C_{4,\chi NN} \sim O(N_c), \tag{13}$$

$$C_{2,\chi NN},\ C_{3,\chi NN} \sim O(\frac{1}{N_c}) \tag{14}$$

(then reduce to independent LECs, $\cdots$). ***Seven independent zero-derivative two-nucleon-DM LECs, three $\sim O(N_c)$, three $\sim O(1)$, one $\sim O(1/N_c)$***.

Low-energy DM-^{3}He Elastic Scatterings

Relevance for future DM direct detection experiment using ^{3}He/^{4}He as targets

- Ratios between DM-light-nuclei cross sections:

$$\frac{\sigma^{\rm SI}_{0,\,^3{\rm He}}}{\sigma^{\rm SD}_{0,\,^3{\rm He}}} \sim O(1) \sim \frac{\sigma^{\rm SI}_{0,\,^3{\rm He}}}{\sigma^{\rm SI}_{0,\,^2{\rm H}}}, \qquad \frac{\sigma^{\rm SD}_{0,\,^3{\rm He}}}{\sigma^{\rm SD}_{0,\,^2{\rm H}}} \sim O(N_c^2), \text{ where SI:} \cdots \left(\chi^\dagger \chi\right), \text{SD:} \cdots \left(\chi^\dagger \sigma^i \chi\right) \tag{15}$$

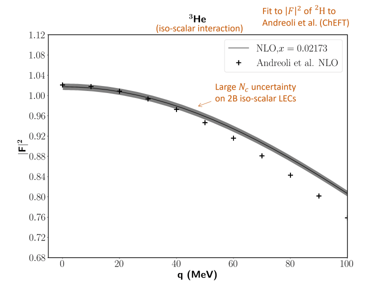

Figure 17: Response function $|F|^2$ of ^{3}He for scalar DM omitting iso-vector interactions. x is fit to $|F|^2$ of deuteron from QMC + ChEFT by *Andreoli, Cirigliano, Gandolfi, and Pederiva 2019*.

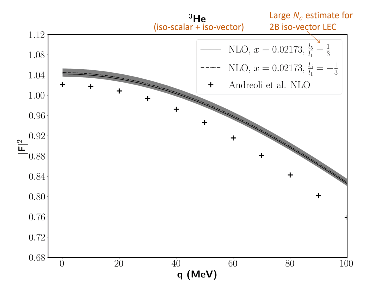

Figure 18: Response function $|F|^2$ of ^{3}He for scalar DM including iso-vector interactions.

Four-Body Systems

Why?

- Four-boson, four-nucleon, four-body nuclear systems, and universalities
- renormalization group behavior of four-body observables and role of Efimov physics

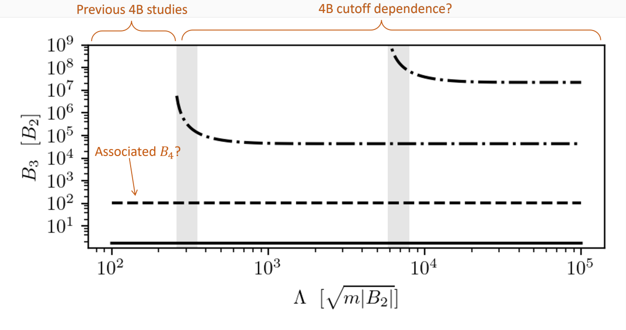

Figure 19: Three-boson binding energies B_3 as a function of cutoff. Previous studies limited to relatively low cutoffs.

Figure 20: Diagrammatic 4B integral equation without 3B force (*Brodsky et al. 2006*)

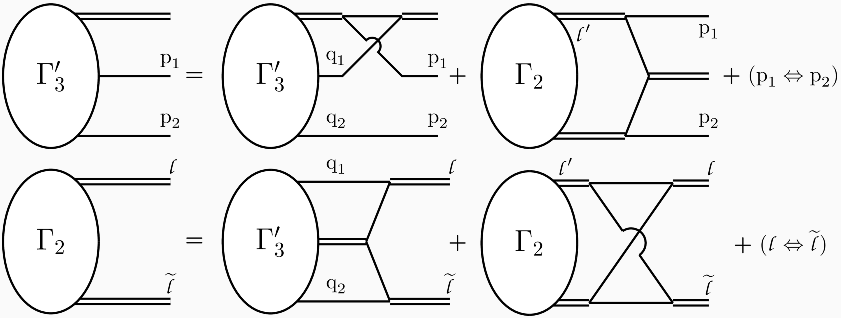

Γ_3': 4-boson amplitude for outgoing dimer-two-single-boson.

Γ_2: 4-boson amplitude for outgoing dimer-dimer states.

- ***3B amplitude and thus 3B bound-state poles do not appear explicitly***

Figure 21: 4B integral equation with 3B amplitudes (*Lin 2023*). t' is half off-shell.

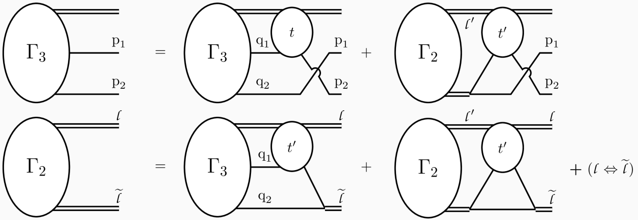

- 3B poles and residues of t can be obtained explicitly using

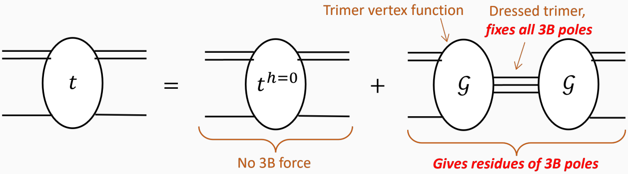

- Use Cauchy's principal value prescription to include/subtract 3B poles. ***Cutoff barrier removed!***

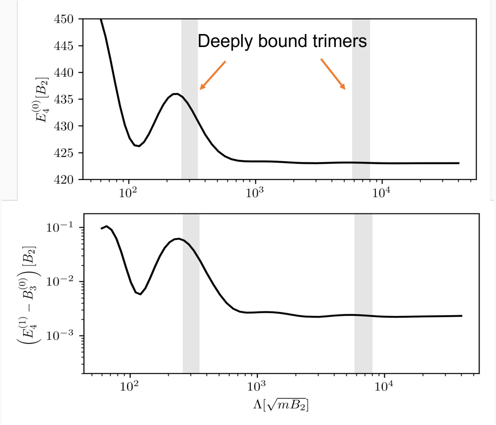

Figure 22: Tetramer binding energies as a function cutoff (*Lin 2023*)

$E_4^{(0)}$: tetramer ground state
$E_4^{(1)}$: tetramer excited state
$B_3^{(0)}$: trimer ground state

- Convergence at $\Lambda \gtrsim 1000\sqrt{mB_2}$

Table 5: Results for cold ^{4}He atoms. Three-boson force fit to the starred (*) value.

	$B_3^{(0)}$ [mK]	$E_4^{(1)}$ [mK]	$E_4^{(0)}$ [mK]
Our results	*128.500	128.503(1)	523.4(5)
Platter et al. 2004	127	128[3]	492[25]
Blume and Greene 2000	125.5	132.7	559.7
Lazauskas and Carbonell 2006	126.39	127.5	557.7

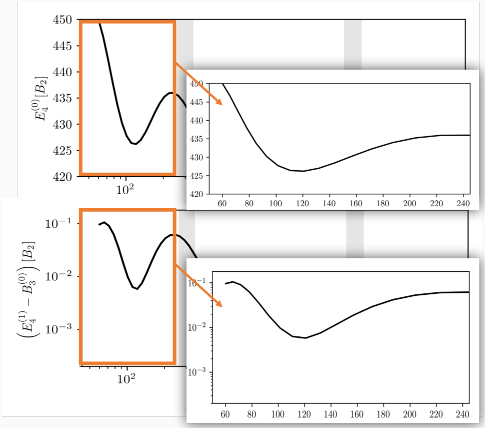

Figure 22: Tetramer binding energies as a function cutoff (*Lin 2023*)

$E_4^{(0)}$: tetramer ground state
$E_4^{(1)}$: tetramer excited state
$B_3^{(0)}$: trimer ground state

- Convergence at $\Lambda \gtrsim 1000\sqrt{mB_2}$
- Misleading plateau at $\Lambda \lesssim 250\sqrt{mB_2}$

Table 5: Results for cold ^{4}He atoms. Three-boson force fit to the starred (*) value.

	$B_3^{(0)}$ [mK]	$E_4^{(1)}$ [mK]	$E_4^{(0)}$ [mK]
Our results	*128.500	128.503(1)	523.4(5)
Platter et al. 2004	127	128[3]	492[25]
Blume and Greene 2000	125.5	132.7	559.7
Lazauskas and Carbonell 2006	126.39	127.5	557.7

Four-Body Results for Cold ^{4}He Atoms

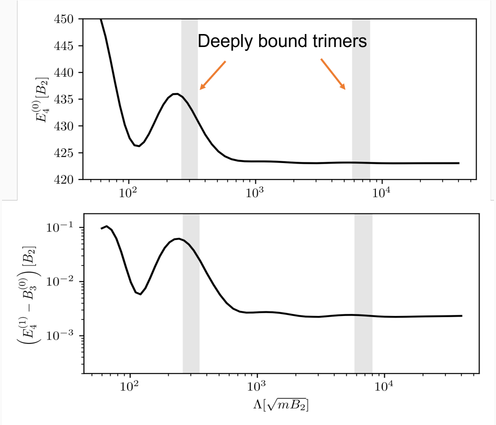

Figure 22: Tetramer binding energies as a function cutoff (*Lin 2023*)

$E_4^{(0)}$: tetramer ground state
$E_4^{(1)}$: tetramer excited state
$B_3^{(0)}$: trimer ground state

- Convergence at $\Lambda \gtrsim 1000\sqrt{mB_2}$
- Misleading plateau at $\Lambda \lesssim 250\sqrt{mB_2}$

Table 5: Results for cold ^{4}He atoms. Three-boson force fit to the starred (*) value.

	$B_3^{(0)}$ [mK]	$E_4^{(1)}$ [mK]	$E_4^{(0)}$ [mK]
Our results	*128.500	128.503(1)	523.4(5)
Platter et al. 2004	127	128[3]	492[25]
Blume and Greene 2000	125.5	132.7	559.7
Lazauskas and Carbonell 2006	126.39	127.5	557.7

Figure 23: Correlations between trimer and tetramer binding energies, Tjon lines (*Tjon 1975*) in nuclear physics. a is the two-boson scattering length.

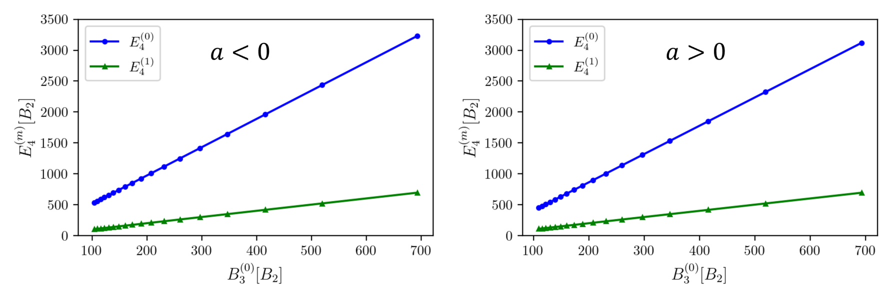

Figure 24: Correlations between $E_4^{(0)}$ and $E_4^{(1)}$ near the unitary limit *Hadizadeh et al. 2011* with our results

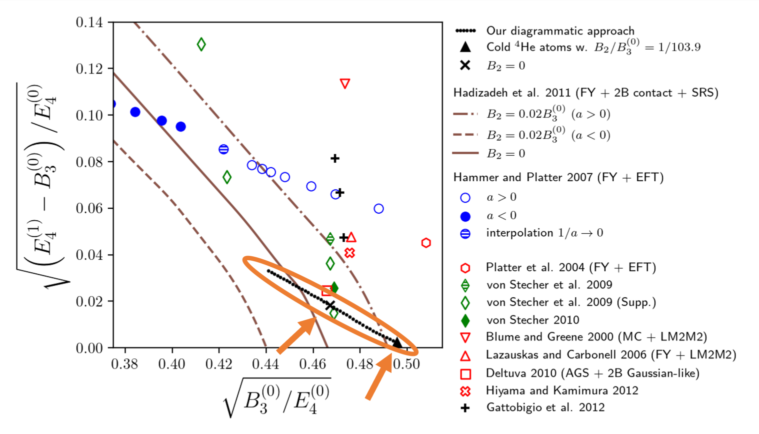

Figure 24: Correlations between $E_4^{(0)}$ and $E_4^{(1)}$ near the unitary limit *Hadizadeh et al. 2011* with our results

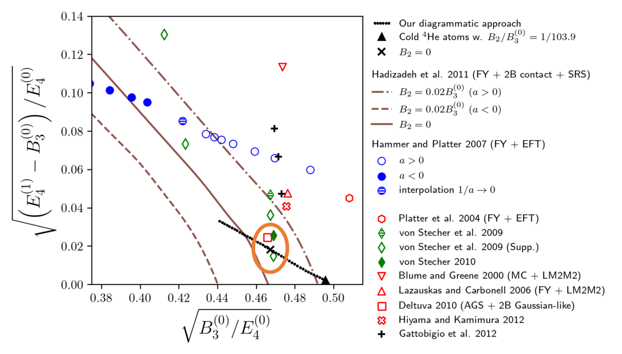

	$E_4^{(0)}/B_3^{(0)}$	$\Gamma_4^{(0)}/(2B_3^{(0)})$	$E_4^{(1)}/B_3^{(0)}$	$\Gamma_4^{(1)}/(2B_3^{(0)})$
Our results	4.58(1)	0.0151(1)	1.0015(3)	$2.06(2) \times 10^{-4}$
Deltuva 2010	4.6108	0.01484	1.00228	2.38×10^{-4}
von Stecher 2010	4.55	-	1.003	-
von Stecher et al. 2009 (Supp., with V_{3b})	4.55	-	1.001	-

Figure 24: Correlations between $E_4^{(0)}$ and $E_4^{(1)}$ near the unitary limit *Hadizadeh et al. 2011* with our results

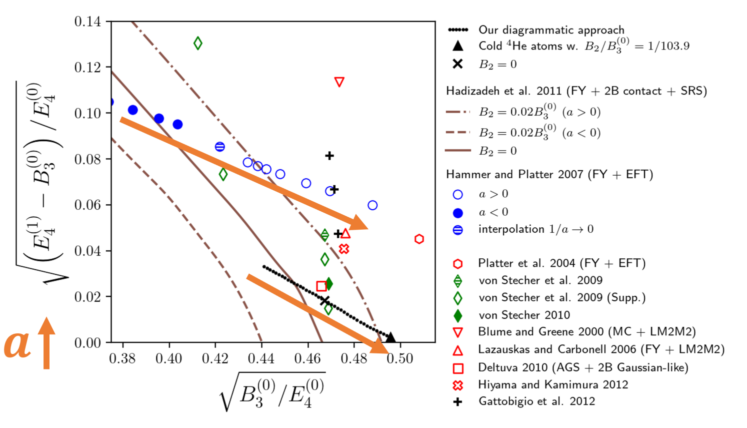

- $E_4^{(1)}$ being close to $B_3^{(0)}$ in the unitary limit carries over to the physical limit of cold ^{4}He atoms.

Summary of what we did:

- 3B systems in Pionless EFT combined with
  - Approximate Wigner-SU(4) symmetry to understand cold *nd* capture and relatively large contribution from multi-nucleon currents. Important because Pionless EFT expansion alone is not sufficient to understand cold *nd* capture, and Wigner-SU(4) symmetry alters its power counting.
  - Large N_c expansion to constrain DM-light-nuclei scatterings. Useful for future DM direct detection experiments using ^{3}He and ^{4}He as targets and help understand the character of DM.
- 4B systems
  - Include/Subtract 3B poles to study RG behavior at large cutoffs. Demonstrated convergence of B_4 at large cutoffs, and verified that no 4B force is needed at LO. Also important for higher-order calculations due to slower convergences there.

Outlook:

- Parity violation in nuclear reactions, e.g., *nd* capture, $n\ ^3$He scattering
- DM-^{4}He scattering with large N_c constraints
- Other four-body systems (e.g., cluster systems) and techniques (e.g., quantum simulation)

Acknowledgement: I would like to thank Jared Vanasse and Roxanne Springer for their support and comments. This material is based upon work supported by the U.S. Department of Energy, Office of Science, Office of Nuclear Physics, under Award Number DE-FG02-05ER41368

References

[1] Xincheng Lin. ***Diagrammatic Approach to Four-Boson Systems in Effective Field Theory.*** 2023. arXiv: 2304.06172 [nucl-th].

[2] Xincheng Lin et al. **"Cold neutron-deuteron capture and Wigner-SU(4) symmetry".** In: *Phys. Rev. C* 108 (4 Oct. 2023), p. 044001. DOI: 10.1103/PhysRevC.108.044001. URL: https://link.aps.org/doi/10.1103/PhysRevC.108.044001.

[3] Thomas R. Richardson, Xincheng Lin, and Son T. Nguyen. **"Large- N_c constraints for elastic dark-matter–light-nucleus scattering in pionless effective field theory".** In: *Physical Review C* 106.4 (Oct. 2022). DOI: 10.1103/physrevc.106.044003. URL: https://doi.org/10.1103%2Fphysrevc.106.044003.

[4] Thomas R. Richardson and Matthias R. Schindler. **"Large-N_c analysis of magnetic and axial two-nucleon currents in pionless effective field theory".** In: *Phys. Rev. C* 101.5 (2020), p. 055505. DOI: 10.1103/PhysRevC.101.055505. arXiv: 2002.00986 [nucl-th].

[5] Lorenzo Andreoli et al. **"Quantum Monte Carlo calculations of dark matter scattering off light nuclei".** In: *Physical Review C* 99.2 (Feb. 2019). DOI: 10.1103/physrevc.99.025501. URL: https://doi.org/10.1103%2Fphysrevc.99.025501.

[6] Bing-Nan Lu et al. **"Essential elements for nuclear binding".** In: *Physics Letters B* 797 (Oct. 2019), p. 134863. DOI: `10.1016/j.physletb.2019.134863`. URL: `https://doi.org/10.1016%2Fj.physletb.2019.134863`.

[7] Jared Vanasse. **"Charge and Magnetic Properties of Three-Nucleon Systems in Pionless Effective Field Theory".** In: *Phys. Rev. C* 98.3 (2018), p. 034003. DOI: `10.1103/PhysRevC.98.034003`. arXiv: `1706.02665 [nucl-th]`.

[8] Jared Vanasse and Daniel R. Phillips. **"Three-nucleon bound states and the Wigner-SU(4) limit".** In: *Few Body Syst.* 58.2 (2017), p. 26. DOI: `10.1007/s00601-016-1173-2`. arXiv: `1607.08585 [nucl-th]`.

[9] Matthias R. Schindler, Roxanne P. Springer, and Jared Vanasse. **"Large-N_c limit reduces the number of independent few-body parity-violating low-energy constants in pionless effective field theory".** In: *Physical Review C* 93.2 (Feb. 2016). DOI: `10.1103/physrevc.93.025502`. URL: `https://doi.org/10.1103%2Fphysrevc.93.025502`.

[10] Jared Vanasse. **"Parity violation in *nd* interactions".** In: *Physical Review C* 86.1 (July 2012). DOI: `10.1103/physrevc.86.014001`. URL: `https://doi.org/10.1103%2Fphysrevc.86.014001`.

[11] M. R. Hadizadeh et al. **"Scaling Properties of Universal Tetramers".** In: *Phys. Rev. Lett.* 107 (13 Sept. 2011), p. 135304. DOI: `10.1103/PhysRevLett.107.135304`. URL: `https://link.aps.org/doi/10.1103/PhysRevLett.107.135304`.

[12] A. Deltuva. **“Efimov physics in bosonic atom-trimer scattering”.** In: *Phys. Rev. A* 82 (2010), p. 040701. DOI: `10.1103/PhysRevA.82.040701`. arXiv: `1009.1295 [physics.atm-clus]`.

[13] Matthias R. Schindler and Roxanne P. Springer. **“Two parity violating asymmetries from n p —> d gamma in pionless effective field theories”.** In: *Nucl. Phys. A* 846 (2010), pp. 51–62. DOI: `10.1016/j.nuclphysa.2010.06.002`. arXiv: `0907.5358 [nucl-th]`.

[14] I. V. Brodsky et al. **“Exact diagrammatic approach for dimer-dimer scattering and bound states of three and four resonantly interacting particles”.** In: *Phys. Rev. A* 73 (3 Mar. 2006), p. 032724. DOI: `10.1103/PhysRevA.73.032724`. URL: `https://link.aps.org/doi/10.1103/PhysRevA.73.032724`.

[15] L. E. Marcucci et al. **“Electromagnetic structure of A=2 and 3 nuclei and the nuclear current operator”.** In: *Phys. Rev. C* 72 (2005), p. 014001. DOI: `10.1103/PhysRevC.72.014001`. arXiv: `nucl-th/0502048`.

[16] J. Formánek, R.J. Lombard, and J. Mareš. **“Wave Equations with Energy-Dependent Potentials”.** In: *Czechoslovak Journal of Physics* 54.3 (Mar. 2004), pp. 289–316. DOI: `10.1023/b:cjop.0000018127.95600.a3`. URL: `https://doi.org/10.1023%2Fb%3Acjop.0000018127.95600.a3`.

[17] Paulo F. Bedaque et al. **“Low energy expansion in the three body system to all orders and the triton channel”.** In: *Nuclear Physics A* 714.3 (2003), pp. 589–610. ISSN: 0375-9474. DOI: *https://doi.org/10.1016/S0375-9474(02)01402-1*. URL: *https://www.sciencedirect.com/science/article/pii/S0375947402014021*.

[18] P.F. Bedaque, H.-W. Hammer, and U. van Kolck. **“The three-boson system with short-range interactions”.** In: *Nuclear Physics A* 646.4 (Feb. 1999), pp. 444–466. DOI: *10.1016/s0375-9474(98)00650-2*. URL: *https://doi.org/10.1016%2Fs0375-9474%2898%2900650-2*.

[19] Jiunn-Wei Chen, Gautam Rupak, and Martin J. Savage. **“Nucleon-nucleon effective field theory without pions”.** In: *Nuclear Physics A* 653.4 (July 1999), pp. 386–412. DOI: *10.1016/s0375-9474(99)00298-5*. URL: *https://doi.org/10.1016%2Fs0375-9474%2899%2900298-5*.

[20] David B. Kaplan, Martin J. Savage, and Mark B. Wise. **“A new expansion for nucleon-nucleon interactions”.** In: *Physics Letters B* 424.3-4 (Apr. 1998), pp. 390–396. DOI: *10.1016/s0370-2693(98)00210-x*. URL: *https://doi.org/10.1016%2Fs0370-2693%2898%2900210-x*.

[21] David B. Kaplan and Martin J. Savage. **"The spin-flavor dependence of nuclear forces from large-N QCD".** In: *Physics Letters B* 365.1-4 (Jan. 1996), pp. 244–251. DOI: *10.1016/0370-2693(95)01277-x*. URL: *https://doi.org/10.1016%2F0370-2693%2895%2901277-x*.

[22] Roger F. Dashen, Elizabeth Ellen Jenkins, and Aneesh V. Manohar. **"Spin flavor structure of large N(c) baryons".** In: *Phys.Rev.* D51 (1995), pp. 3697–3727. DOI: *10.1103/PhysRevD.51.3697*.

[23] E. T. Jurney, P. J. Bendt, and J. C. Browne. **"Thermal neutron capture cross section of deuterium".** In: *Phys. Rev. C* 25 (1982), pp. 2810–2811. DOI: *10.1103/PhysRevC.25.2810*.

[24] D. D. Faul et al. **"Photodisintegration of ^{3}H and ^{3}He".** In: *Phys. Rev. C* 24 (3 Sept. 1981), pp. 849–873. DOI: *10.1103/PhysRevC.24.849*. URL: *https://link.aps.org/doi/10.1103/PhysRevC.24.849*.

[25] Edward Witten. **"Baryons in the 1/n Expansion".** In: *Nucl. Phys. B* 160 (1979), pp. 57–115. DOI: *10.1016/0550-3213(79)90232-3*.

[26] J.A. Tjon. **"Bound states of 4He with local interactions".** In: *Physics Letters B* 56.3 (1975), pp. 217–220. ISSN: 0370-2693. DOI: *https://doi.org/10.1016/0370-2693(75)90378-0*. URL: *https://www.sciencedirect.com/science/article/pii/0370269375903780*.

[27] Gerard 't Hooft. **"A Planar Diagram Theory for Strong Interactions".** In: *Nucl. Phys. B* 72 (1974). Ed. by J. C. Taylor, p. 461. DOI: *10.1016/0550-3213(74)90154-0*.

[28] E. Wigner. **"On the Consequences of the Symmetry of the Nuclear Hamiltonian on the Spectroscopy of Nuclei".** In: *Phys. Rev.* 51 (2 Jan. 1937), pp. 106–119. DOI: *10.1103/PhysRev.51.106*. URL: *https://link.aps.org/doi/10.1103/PhysRev.51.106*.

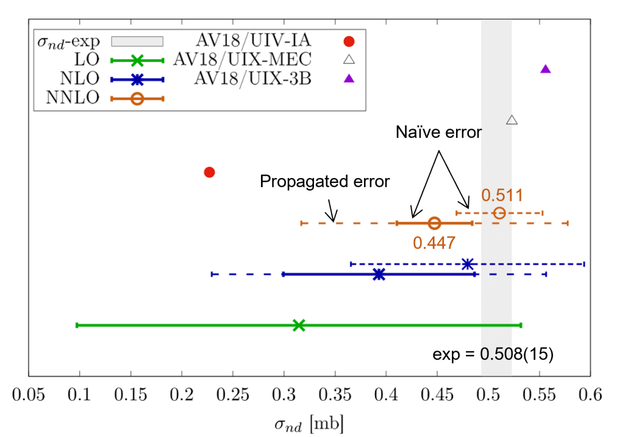

Figure 24: Pionless EFT results compared with potential model calculations (*Marcucci et al. 2005*) and experiment (*Jurney, Bendt, and Browne 1982*). Solid and short dashed lines represent errors from naive pionless EFT expansion. Long dashed lines represent propagated errors from $L_1^{(0)/(1)}$ fit.

Naive error of an observable at m-th order (denoted O_m):

$$\Delta_N(\mathcal{O}_m) = \left|\beta Q^{m+1}\mathcal{O}_m\right| \tag{16}$$

where the subscript “N” indicates “naive” error. Suppose a LEC C_m at m-th order is fit to the experimental value of the observable ($O^{\exp}$), the error above can be propagated to C_m:

$$\begin{aligned}\Delta C_m &= \left|\frac{\Delta_N(\mathcal{O}_m)}{\partial\mathcal{O}_m/\partial C_m}\right| \\ &= \left|\frac{\beta Q^{m+1}\mathcal{O}^{\exp}}{\partial\mathcal{O}_m/\partial C_m}\right|,\end{aligned} \tag{17}$$

Calculating a different observable O'_m using this C_m will lead to an error on O'_m:

$$\Delta_P(\mathcal{O}'_m) = \left|\frac{\partial\mathcal{O}'_m}{\partial C_m}\right|\Delta C_m \tag{18}$$

where the subscript “P” indicates “propagated” error

Preliminary Results of E1 Contributions

- One-, two-, and three-nucleon currents obtained from gauging kinetic terms

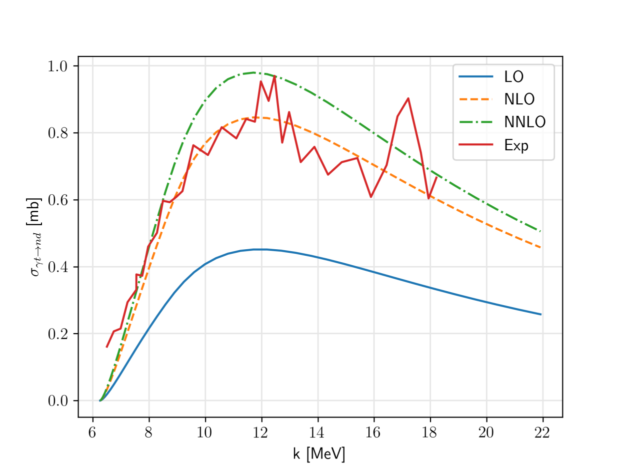

Figure 25: Preliminary results on triton photo-disintegration cross section as a function of photon energy. Experimental data from *Faul, Berman, Meyer, and Olson 1981*.

Consider one-quark operator,

$$S^i = q^\dagger \frac{\sigma^i}{2} q,\ I^a = q^\dagger \frac{\tau^a}{2} q,\ G^{ia} = q^\dagger \frac{\sigma^i}{2}\frac{\tau^a}{2} q. \tag{19}$$

For physical baryon, the large N_c scaling of their single-baryon matrix elements is given by

$$\langle B| S^i |B\rangle \sim \langle B| I^a |B\rangle \sim O(1) \tag{20}$$